AIAA JOURNAL
Vol. 40, No. 2, February 2002

Computation of Flow Noise Using Source Terms in Linearized Euler's Equations

Christophe Bogey,* Christophe Bailly,† and Daniel Juvé‡
Ecole Centrale de Lyon, 69131 Ecully, France

An acoustic analogy using linearized Euler's equations (LEE) forced with aerodynamic source terms is investigated to compute the acoustic far field. This hybrid method is applied to three model problems simulated by solving Navier–Stokes equations. In this way, its validity is estimated by comparing the predicted acoustic field with the reference solution given directly by the Navier–Stokes equations. The noise radiated by two corotating vortices is studied: first, in a medium at rest and, second, in a mean sheared flow with no convection velocity. Then the sound field generated by vortex pairings in a subsonic mixing layer is investigated. In this case, a simplified formulation of LEE is proposed to prevent the exponential growth of instability waves. The acoustic fields obtained by solving LEE are in good agreement with the reference solution. This study shows that the source terms introduced into the LEE are appropriate for free sheared flows and that acoustic–mean flow interactions are properly taken into account in the wave operator.

Nomenclature

b	=	half-width of the monopolar source
c	=	sound velocity
$\boldsymbol{E}, \boldsymbol{F}, \boldsymbol{H}$	=	vectors in linearized Euler's equations (LEE)
f	=	frequency
f_0	=	fundamental frequency of the mixing layer
k	=	complex wave number, $k_r + ik_i$
M	=	Mach number
p	=	pressure
Re	=	Reynolds number
r_c	=	vortex core radius
r_0	=	initial half distance between the two vortices
$\boldsymbol{S}$	=	sound source vector in LEE
S_i	=	source terms in the momentum equations
T	=	period
T_{ij}	=	Lighthill's tensor
t	=	time
$\boldsymbol{U}$	=	unknown vector in LEE
U_1	=	slow stream velocity of the mixing layer
U_2	=	rapid stream velocity of the mixing layer
$\boldsymbol{u}$	=	velocity vector, (u_1, u_2)
V_θ	=	initial tangential velocity of vortices
x	=	radial distance, $\sqrt{(x_1^2 + x_2^2)}$
$\boldsymbol{x}$	=	Cartesian coordinate vector, (x_1, x_2)
$\boldsymbol{y}$	=	Cartesian coordinate vector
Γ	=	vortex circulation
γ	=	specific heat ratio
Δ	=	grid size
Δt	=	time step
ΔU	=	velocity of the two opposite streams for the sheared mean flow
δ_ω	=	vorticity thickness
ϵ	=	amplitude of the monopolar source
Θ	=	dilatation, $\nabla \cdot \boldsymbol{u}$
Λ	=	source term in Lilley's equation
λ	=	acoustic wavelength
ν	=	kinematic molecular viscosity
ρ	=	density
ω	=	angular frequency

Subscripts

a	=	acoustic
i, j	=	indices
p	=	pairing
r	=	rotation
0	=	ambient

Superscripts

t	=	vector transpose
$'$	=	fluctuating value
$\bar{}$	=	mean value

Received 13 March 2001; revision received 29 June 2001; accepted for publication 2 July 2001.

*Research Scientist, Laboratoire de Mécanique des Fluides et d'Acoustique, UMR Centre National de la Recherche Scientifique 5509, B.P. 163; christophe.bogey@ec-lyon.fr. Member AIAA.

†Assistant Professor, Laboratoire de Mécanique des Fluides et d'Acoustique, UMR Centre National de la Recherche Scientifique 5509, B.P. 163; christophe.bailly@ec-lyon.fr. Member AIAA.

‡Professor, Laboratoire de Mécanique des Fluides et d'Acoustique, UMR Centre National de la Recherche Scientifique 5509, B.P. 163. Member AIAA.

I. Introduction

RECENT and spectacular achievements of computational aeroacoustics (CAA) in aerodynamic noise prediction are based on the direct calculation of the acoustic field by solving the unsteady compressible Navier–Stokes equations. Carrying on the work of the Stanford research group, Freund[1] has performed the direct numerical simulation (DNS) of a Mach number $M = 0.9$ jet with a Reynolds number based on the jet diameter $Re = 3.6 \times 10^3$, providing directly an acoustic far field conformable to measurements. Direct computation of the noise radiated by a subsonic three-dimensional jet, however, remains difficult because of the large computing resources required and also because of numerical issues inherent in CAA. In DNS, all turbulent scales, namely, from the integral length scale to Kolmogorov's scale, are to be described. Colonius[2] has estimated the cost of a DNS of a subsonic turbulent jet providing both local flowfield and acoustic field: The total cost of an efficient numerical algorithm is proportional to Re^3/M^4. In the same manner, the cost of a direct acoustic calculation using a large-eddy simulation (LES), assuming that the size of the resolved smallest eddies is given by the Taylor length scale, is proportional to Re^2/M^4. In that way, Bogey[3] and Bogey et al.[4] have calculated directly by LES the noise radiated by a Mach 0.9 jet with a Reynolds number $Re = 6.5 \times 10^4$.

Direct calculation of noise is quite expensive for flows of practical interest with high Reynolds numbers and often moderate Mach numbers. In many engineering problems, only the time-dependent flowfield can be determined. To investigate the sound field in this case, a hybrid method is necessary. It consists in separating the treatments of sound generation and of sound propagation. Among the

first hybrid methods, the most famous is based on Lighthill's wave equation,[5] simply derived from the conservation laws of motion. The acoustic field is then obtained by solving a classical wave equation in which the source term is written as a function of the local flowfield. A difficulty of Lighthill's equation is the interpretation of the source term where mean flow effects on the wave propagation are included.[6] Therefore, to take into account all of these effects, application of Lighthill's equation requires a source volume containing all acoustic–flow interactions and not only the turbulent region.[7] With this in view, the velocity field used to build up source terms must be compressible.

To describe acoustic propagation exactly in unidirectional sheared mean flows, a third-order wave operator was developed, particularly by Lilley[8] and Pridmore-Brown.[9] The associated source term is mainly a nonlinear function of the fluctuating velocity flowfield. Many studies have been devoted to the resolution of Lilley's equation: analytically,[10] by using geometrical methods,[11] or more recently, numerically.[12] A time resolution can be performed by transforming Lilley's equation into a system of first-order equations. In this way, Berman and Ramos[13] have calculated the radiation of a monopolar source in a jet mean flow provided by a Navier–Stokes code with k–ϵ turbulent closure. This idea was developed by Béchara et al.[14] with an approach using linearized Euler's equations (LEE), which account for refraction and convection effects in any sheared mean flows. In this approach, a source term is added into the right-hand side of LEE and is built up from a synthesized turbulent field. The source term expression and the construction of a stochastic space-time turbulent field were improved later[15] and extended to three-dimensional geometries.[16,17]

The primary objective of this paper is to show that an acoustic analogy combining LEE with the source terms defined by Bailly et al.[15] is able to predict aerodynamic noise. The validity of this hybrid approach is checked by investigating the sound radiation for three flow configurations, in the following way. First, a reference solution of the acoustic far field is determined directly from the Navier–Stokes equations. The local flowfield of this simulation is then used to build up the source terms introduced into LEE and to estimate the mean flow. Finally, the acoustic field obtained by solving LEE is compared to the reference solution to evaluate the accuracy of the hybrid approach, with regard to both the expression of source terms and acoustic–mean flow interactions. LEE support both acoustic disturbances and instability waves, which are not decoupled in a sheared mean flow. As a result, physical growing instability waves can be excited by the source terms. We then propose to remove this coupling by considering a simplified formulation of LEE, without significant effects on noise propagation.

In Sec. II, we present the formulation of the source terms introduced in two-dimensional LEE. Next, three building block problems are considered. Sound field generated by two corotating vortices in a medium at rest is studied in Sec. III. In Sec. IV, the same problem is investigated in the presence of a sheared mean flow with zero convection velocity. In this way, development of instability waves is neutralized. The noise generated by a mixing layer is then investigated in Sec. V. Influence of some quantities, such as the mean value of source terms, and the removal of instability waves are also discussed. Definition of source terms for LEE and connection with Lilley's equation are given in Appendix A. An analysis of simplified LEE is shown in Appendix B, and a sound propagation problem is solved in Appendix C using the physical parameters of the mixing layer.

II. Hybrid Method Based on LEE

A. Formulation

Consider small perturbations around a steady mean flow with density $\bar{\rho}$, velocity $\bar{\boldsymbol{u}} = (\bar{u}_1, \bar{u}_2)$, and pressure $\bar{p}$. The behavior of these perturbations is governed by LEE, written in a two-dimensional conservative form, as

$$\frac{\partial \boldsymbol{U}}{\partial t} + \frac{\partial \boldsymbol{E}}{\partial x_1} + \frac{\partial \boldsymbol{F}}{\partial x_2} + \boldsymbol{H} = \boldsymbol{S} \tag{1}$$

where $\boldsymbol{U} = [\rho', \bar{\rho}u_1', \bar{\rho}u_2', p']^t$ is the unknown vector. The prime denotes the perturbation variable. Complete expressions of vectors $\boldsymbol{E}$, $\boldsymbol{F}$, and $\boldsymbol{H}$ are given in Appendix A, and $\boldsymbol{S}$ represents a possible source term.

Assuming isentropic flows, noise generation is provided by source terms in the momentum equations of LEE. Additional source terms will be required to take into account entropic sound sources. In the present hybrid approach, vector $\boldsymbol{S}$ is written as[15]

$$\boldsymbol{S} = \begin{bmatrix} 0 \\ S_1 - \overline{S_1} \\ S_2 - \overline{S_2} \\ 0 \end{bmatrix}$$

where

$$S_i = -\frac{\partial \rho u_i' u_j'}{\partial x_j}, \qquad \overline{S_i} = -\overline{\frac{\partial \rho u_i' u_j'}{\partial x_j}} \tag{2}$$

This expression of source terms S_i in LEE is found by analogy with Lilley's equation: The reasoning used is presented in Appendix A. The source terms S_i are nonlinear in velocity fluctuations, and their mean values $\overline{S_i}$ are subtracted. The motivations for the latter point will be presented in the test cases reported in the present paper. Data provided by incompressible or compressible simulations can be used to estimate S_i. In the compressible case, however, the acoustic field is included in the source terms, through density and fluctuating velocity, but this acoustic component is very small compared to aerodynamic fluctuations. The cross terms involving acoustic and aerodynamic perturbations are associated to sound scattering by turbulence, which is generally small. Note that using the mean density value instead of the instantaneous one does not matter because the terms $\rho' u_i' u_j'$ involving three fluctuating quantities are negligible.

For the three applications presented in Secs. III–V, the Navier–Stokes equations are solved using the ALESIA code to obtain the reference acoustic far field. LEE are then solved separately by the SPRINT code, using the mean velocity field and source terms (2) evaluated from the Navier–Stokes computation, and the resulting acoustic field is compared to the reference solution. The two solvers will be briefly described in the next subsections. Source terms calculated from the Navier–Stokes simulation are stored once the flow is well established, into files around 200 megaoctets. The recording time is long enough that the sound radiation given by LEE can propagate in the whole computational domain and that a possible initial acoustic transient can exit. It also contains several flow periods so that the mean source terms converge. In the Navier–Stokes and LEE simulations performed in this work, computational domains are similar to allow the comparison between the two computed sound fields. CPU time and memory requirements are, thus, of the same order. For the two corotating vortices, the grids are identical, and the numerical efficiency is the same. However, for the mixing layer case, where only every other point of the LES grid is kept for LEE, the resolution of LEE is eight times more efficient. More generally, the gains realized with the hybrid approach are important when the grid used for solving LEE is coarser than the Navier–Stokes grid.

B. Flow Simulation

A two-dimensional and three-dimensional code, ALESIA, solving unsteady compressible Navier–Stokes equations has been developed[3] to provide directly both the local flowfield and the radiated sound field. It can be run to perform DNS. A turbulence modeling is also implemented to carry out LES of flows at a high Reynolds number. In this case, only the larger structures are resolved, and effects of the smaller scales are taken into account via the Smagorinsky subgrid-scale model. Equations are solved in a conservative form on a Cartesian grid. The space derivatives are discretized with the dispersion-relation-preserving (DRP) scheme of Tam and Webb,[18] and the time integration is performed by a fourth-step Runge–Kutta algorithm. Great care is taken to exploit directly the computed acoustic field. The nonreflecting boundary conditions of Tam and Dong,[19] based on the asymptotic expression of Euler's equations in the far field, are implemented. Outflow boundary conditions combined with a sponge zone are used to allow the exit of vortical structures without generating significant spurious waves. More details are given by Bogey[3] and Bogey et al.[20]

C. Resolution of LEE

A two- and three-dimensional LEE solver, SPRINT, has been built using CAA techniques.[21] An outline of the numerical procedure will follow. LEE are solved using the DRP scheme of Tam and Webb[18] to evaluate spatial derivatives. The solution is advanced in time with a fourth-order Runge–Kutta integration. The radiation and outflow boundary conditions are based on the asymptotic formulation of LEE[19] in the acoustic far field. A sponge zone is also used when linear instability waves are convected by the mean flow to dissipate aerodynamic fluctuations and to avoid the generation of acoustic reflections at the outflow boundary.

III. Sound Field Generated by Two Corotating Vortices in a Medium at Rest

A. Flow Simulation

In this first application, the noise generated by two corotating vortices in a medium at rest is investigated. The initial tangential velocity distribution of each vortex is given by the following expression[22]:

$$V_\theta(r) = -\frac{\Gamma r}{2\pi\left(r_c^2 + r^2\right)}$$

where r is the radial distance from the vortex center. The two vortices are separated by a distance of $2r_0$, as shown in Fig. 1. The angular frequency of the whole swirling flow is[23] $\omega_r = 2\pi f_r = \Gamma/(4\pi r_0^2)$, the period is $T_r = 8\pi^2 r_0^2/\Gamma$, and the rotation Mach number is $M_r = \Gamma/(4\pi r_0 c_0)$. In this study, the Mach number based on the maximum tangential velocity $\Gamma/(4\pi r_c)$ is 0.5, $r_c/r_0 = \frac{2}{9}$, $M_r = \frac{1}{9}$, and the Reynolds number $Re = \Gamma/\nu$ is 1.14×10^5.

The acoustic field is calculated directly by a DNS using ALESIA without turbulence modeling. The square computational mesh has 281×281 points with a regular step size $\Delta = r_0/18$ for the first 30 points in each direction from the mesh center and extends to $104r_0$. The time step is $\Delta t = 0.8\Delta/c_0$, which gives a rotation period $T_r \simeq 1272\Delta t$. The acoustic source associated with the two vortices is a rotating quadrupole,[23] and the acoustic frequency is $f_a = 2 \times f_r$ because of the source symmetry. The mesh is stretched so that at least seven points are in the acoustic wavelength $\lambda_a = 28.3r_0$. The simulation runs for 12×10^3 iterations.

As described by Mitchell et al.,[24] the two vortices have a time period of corotation, during $6T_r$, before a sudden merger. Then the two cores coalesce with production of vorticity filaments and finally evolve into a single circular vortex. The resulting sound field during the corotation period is, after a transient wave, an acoustic radiation at the frequency f_a. The amplitude of the acoustic signal increases when the vortices begin to merge and reaches a peak when they coalesce. After merger, it diminishes significantly.

A snapshot of the near field dilatation $\Theta = \nabla \cdot \boldsymbol{u}$ during the corotation period is shown in Fig. 2. The dilatation is directly connected to the time derivative of the acoustic pressure in a medium at rest by the relation $\Theta = -1/(\rho_0 c_0^2)\partial p/\partial t$. The use of the dilatation as acoustic variable allows getting rid of the low-frequency small drift of the mean pressure field.[12] There is actually no pressure drift in this first application, but dilatation will be used to represent the acoustic field in all of the paper. The typical double spiral pattern of a rotating quadrupolar source, found analytically by Powell[23] and numerically by Lee and Koo[22] and Mitchell et al.,[24] is obtained.

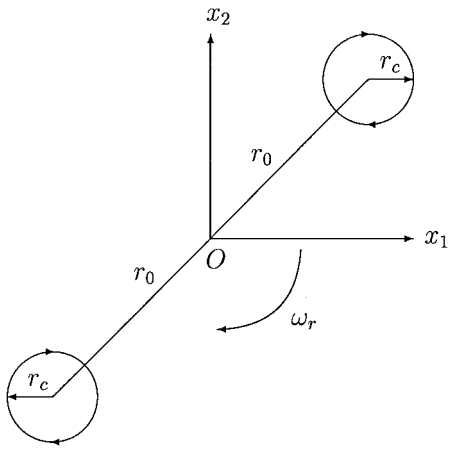

Fig. 1 Two corotating vortices.

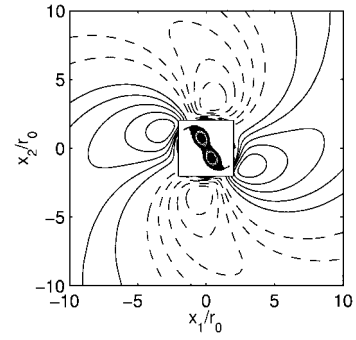

Fig. 2 Two corotating vortices in a medium at rest; snapshot of the near vorticity field surrounded by seven isocontours of the dilatation field defined from 8 to 56 s^{-1} with constant increment: ——, positive values and – – –, negative values.

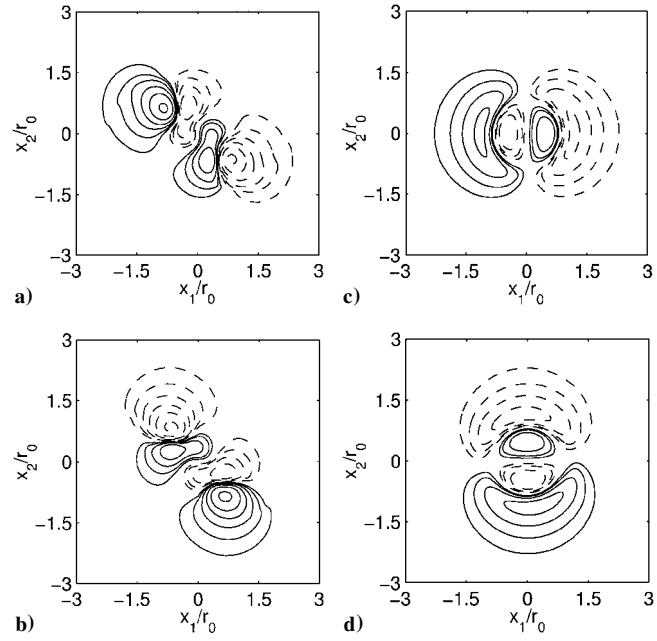

Fig. 3 Two corotating vortices in a medium at rest; representation of source terms; ——, positive values and – – –, negative values: a) S_1 and b) S_2 with six contours from 6×10^5 to $1.1 \times 10^7 s^{-1}$ following a geometrical ratio of 1.8, and c) $\overline{S_1}$ and d) $\overline{S_2}$ with the first four contours defined earlier from 6×10^5 to 3.5×10^6 s^{-1}.

B. Application of LEE

1. Source Terms

Aerodynamic fluctuations provided by the DNS are now used to build up the source terms (2). They are recorded every iteration from $t = 2000\Delta t$ to $6000\Delta t$, on a square domain of size $9.5r_0$ corresponding to an 121×121 grid, and stored into 240-megaoctet files. The source domain is large enough to avoid significant truncation of the source terms. Their amplitudes on the boundaries are less than 1% of their maximum amplitude reached in the source domain. LEE (1) are then solved on the same mesh as the earlier DNS, with the same time step because the numerical algorithms are identical.

The two source term components, instantaneous S_i and average $\overline{S_i}$ calculated from the 4000 recording time steps, are shown in Fig. 3. The value of the average of the source terms is not negligible, of the order of one-third of the value of the instantaneous source terms. LEE are solved with source terms S_i, then with $S_i - \overline{S_i}$. The two dilatation profiles obtained in this way at $t = 2800\Delta t$ are presented in Fig. 4. The main difference is that an acoustic transient signal with amplitude higher than one of physical radiation is observed by using S_i but not with $S_i - \overline{S_i}$. This transient may generate spurious waves when hitting the boundaries: Centering the source terms introduced into LEE allows avoiding this numerical difficulty.

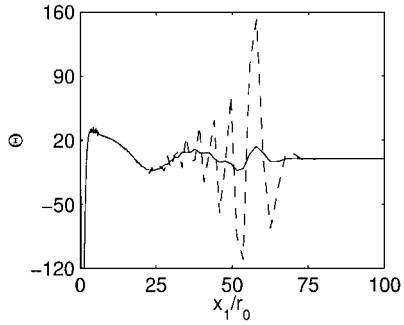

Fig. 4 Two corotating vortices in a medium at rest. Dilatation profiles obtained at $t = 2800\Delta t$, in s^{-1}, at $x_2 = 0$ with $x_1 > 0$, by solving LEE, with source terms: - - -, S_i and ——, $S_i - \overline{S_i}$.

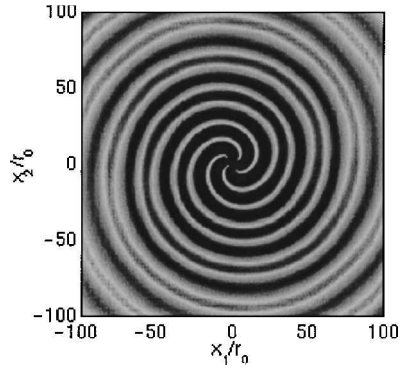

Fig. 5 Noise generated by two corotating vortices in a medium at rest; snapshot of the dilatation field obtained at $t = 6000\Delta t$ by solving LEE with source terms (2), levels from − 15 to 15 s^{-1}.

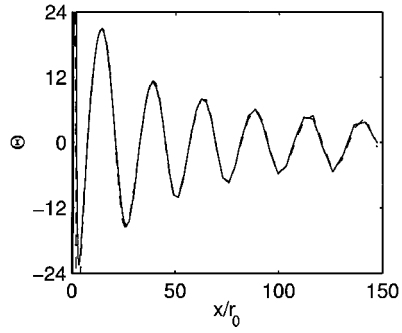

Fig. 6 Two corotating vortices in a medium at rest; dilatation profiles obtained at $t = 6000\Delta t$, s^{-1}, along the line $x_1 = x_2$ with $x_1 > 0$: - - -, by solving LEE with source terms (2) and ——, by DNS.

2. Results

The dilatation field predicted by LEE at $t = 6000\Delta t$ is presented in Fig. 5. It is in good agreement with the reference solution.[3] To provide a more quantitative comparison, dilatation profiles obtained by solving LEE and from the DNS are shown in Fig. 6, and they are superposable. This simple example shows that the acoustic analogy based on LEE with the source term (2) is able to provide correctly the radiated acoustic field when there is no mean flow and thus no acoustic–mean flow interactions. In this case, the result obtained by solving Lighthill's equation with the same source region would have been the same.

IV. Sound Field Generated by Two Corotating Vortices in a Sheared Mean Flow

A. Flow Simulation

To study how mean flow effects on propagation are accounted for by the hybrid method, the vorticity distribution defined earlier in Sec. III, consisting of two corotating vortices, is simply superimposed on a sheared mean flow with a zero convection velocity,

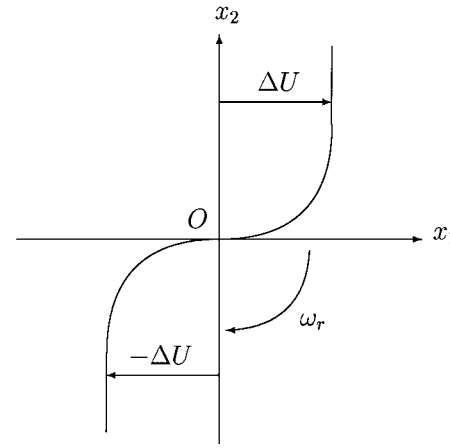

Fig. 7 Sheared mean flow with a zero convection velocity; two flow velocities ± ΔU and rotation of two corotating vortices shown by ω_r.

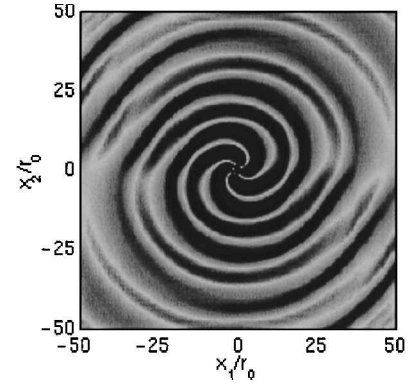

Fig. 8 Two corotating vortices placed in a sheared mean flow; snapshot of the dilatation field obtained at $t = 2500\Delta t$ by DNS; levels from − 50 to 50 s^{-1}.

shown in Fig. 7. The following hyperbolic tangent profile is chosen for the mean flow:

$$\bar{u}_1(x_2) = \Delta U \tanh(2x_2/\delta_\omega) \tag{3}$$

with $\Delta U = 0.125c_0$. The vorticity thickness is taken as $\delta_\omega = 4r_0$, where r_0 is half the distance between the two vortices. Thus, the Reynolds number based on the velocity difference $2\Delta U$ and the vorticity thickness is 0.816×10^5. Mean density and mean pressure are constant. The acoustic reference solution is again calculated directly by DNS. The middle part of the mesh given in Sec. III.A is used to obtain a Cartesian grid of 251×251 points, which extends to $55r_0$ in each direction.

The vorticity field shows the usual steps of the merging process, given earlier in Sec. III.A: a time of corotation of the two vortices, followed by a sudden merger, and finally by the formation of a single circular vortex. In this configuration, however, the rotation induced by the sheared mean flow is added to the natural rotation of the two spinning vortices. Thus, the period of rotation is smaller, $T_r \simeq 750\Delta t$, and corresponds to an acoustic wavelength of $\lambda_a \simeq 16.7r_0$. Moreover, there are only three periods of corotation before the merger. The dilatation field obtained by DNS at time $t = 2500\Delta t$ is shown in Fig. 8. The dilatation variable is related to the acoustic pressure by

$$\Theta = -\frac{1}{\rho_0 c_0^2}\left(\frac{\partial p}{\partial t} \pm \Delta U \frac{\partial p}{\partial x_1}\right)$$

for the upper stream and lower stream, respectively. In comparison with Fig. 6, wave fronts are ovalized due to mean flow convection effects. There are also refraction effects, but they are not important because the shear layer vorticity thickness $4r_0$ is small with respect to the acoustic wavelength λ_a.

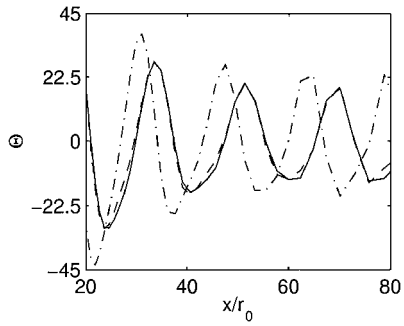

Fig. 9 Two corotating vortices placed in a sheared mean flow; dilatation profiles obtained at $t = 2500\Delta t$, s^{-1}, along the line $x_1 = x_2$ with $x_1 > 0$, by solving LEE with source terms (2): – – –, with mean flow, – · – · –, without mean flow, and ——, by DNS.

B. Application of LEE

Source terms are recorded every iteration between $t = 200\Delta t$ and $2500\Delta t$ on the same square domain as in Sec. III.2, and stored into 130-megaoctet files. LEE are solved by using the analytic mean velocity profile (3). The transverse mean velocity is zero and mean pressure and density are taken to be constant, with the same values used to initialize the DNS. No instability wave is observed because the shear flow has no convection velocity. It is numerically very favorable because the exponential growth of instability waves classically found in a uniform shear flow would have made the noise calculation impossible.

The dilatation field predicted by solving LEE is consistent with the DNS field shown in Fig. 8. The dilatation profile obtained along a diagonal line of the computational domain is plotted in Fig. 9, and it is in very good agreement with the DNS profile. Acoustic–mean flow interactions are, thus, properly taken into account in the LEE. The importance of mean flow effects on wave propagation in this flow configuration can be underlined by solving LEE without mean velocity field, by setting $\bar{u}_1 = 0$. This is clearly illustrated by the corresponding dilatation profile shown in Fig. 9, which is wrong in amplitude and in phase.

V. Sound Field Generated by a Mixing Layer

A. Flow Simulation

In this last application, the noise generated by a subsonic mixing layer between two flows at $U_1 = 40$ and $U_2 = 160$ m · s^{-1} is studied, the sound velocity being $c_0 \simeq 340$ m · s^{-1} (Fig. 10). The mixing layer corresponds to a more general flow than the two earlier configurations. The inflow hyperbolic tangent profile is given by

$$u_1(x_2) = (U_1 + U_2)/2 + [(U_2 - U_1)/2]\tanh[2x_2/\delta_\omega(0)] \quad (4)$$

where $\delta_\omega(0)$ is the initial vorticity thickness. One also defines the convection velocity as $U_c = (U_1 + U_2)/2 = 100$ m · s^{-1}, and the Reynolds number $Re = (U_2 - U_1)\delta_\omega(0)/\nu = 1.28 \times 10^4$. The flow is forced at its fundamental frequency f_0 and its first subharmonic $f_0/2$ to fix the location of vortex pairings in the mixing layer around $x_1 \simeq 70\delta_\omega(0)$. The acoustic field is calculated directly by a LES using ALESIA. Details of the simulation as well as acoustic results and comparisons with Lighthill's analogy can be found in Bogey[3] and Bogey et al.[7,20] The dilatation field is shown in Fig. 11 on the whole physical computational domain. Wave fronts are observed coming from the location of pairings with an acoustic wavelength $\lambda_p = 51.5\delta_\omega(0)$, corresponding to the frequency of pairings $f_p = f_0/2$. Convection effects are visible and are well marked in the upper rapid flow.

B. Application of LEE

1. Source Terms

The source region extends from $5\delta_\omega(0)$ to $235\delta_\omega(0)$ in the axial direction and from $-50\delta_\omega(0)$ to $50\delta_\omega(0)$ in the transversal direction. The mesh used in the source region is coarser because only every other point of the LES grid in the two coordinate directions is kept. Source terms are recorded every other time step, during the last 5400 LES iterations corresponding to 16 pairing periods, and stored into 250-megaoctet files. In this way, $\Delta t_{\mathrm{LEE}} = 2\Delta t_{\mathrm{LES}}$, and space or time interpolations of source terms are avoided. The mean velocity field is provided by the LES, whereas mean density and pressure are constant. Figure 12 shows the mean axial velocity contours in the shear flow region and shows clearly the location of vortex pairings around $x_1 \simeq 70\delta_\omega(0)$ with a doubling of the shear layer thickness.

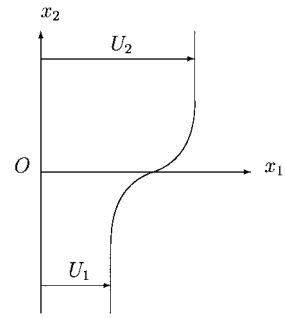

Fig. 10 Mixing layer; two flow velocities U_1 and U_2.

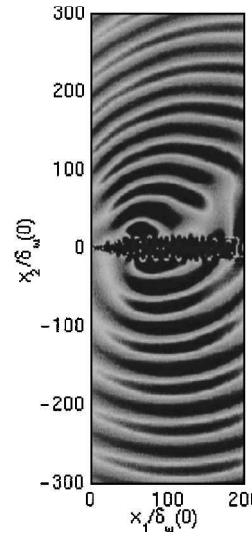

Fig. 11 Noise generated by a mixing layer; snapshot of the dilatation field obtained by LES, levels from − 1.6 to 1.6 s^{-1}.

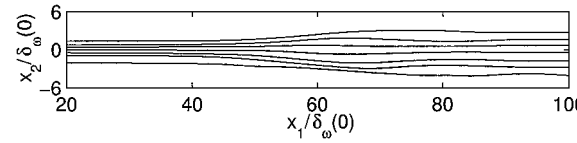

Fig. 12 Mean axial velocity contours obtained by LES in the mixing layer; contours from bottom to top: 44, 52, 68, 100, 132, 148, and 156 m · s^{-1}.

2. Simplified Formulation of LEE

Growing instability waves are excited by source terms introduced into LEE, through the mean shear $\partial\bar{u}_1/\partial x_2$ in the vector $\boldsymbol{H}$ (see expression in Appendix A). To prevent the exponential development of linear instability waves, we set $\boldsymbol{H} = 0$. This simplified formulation of LEE allows us to consider only the acoustic mode (see Appendix B for a discussion of this assumption). A test case is also performed in Appendix C to show that acoustic propagation is not significantly modified in the case of a monopolar source at frequency f_p placed in the mean velocity field of the mixing layer.

3. Contribution of the Average of Source Terms

The source terms in Eq. (2) are decomposed as $S_i - \overline{S_i}$. The two components S_i and $\overline{S_i}$ are presented in Fig. 13, and they have similar amplitude. To investigate the contribution of the average of the source terms to the pressure field, in addition to the acoustic transient found in the first application, LEE are solved with the mean velocity field taken as zero and with three source terms, $S_i - \overline{S_i}$, S_i, and $\overline{S_i}$ successively. Figure 14 shows the transverse pressure profiles found with the three source terms. The time average of the source terms generates a steady pressure field.

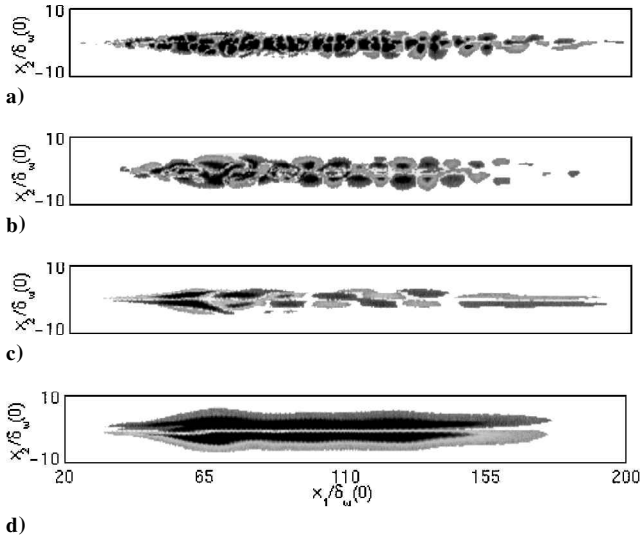

Fig. 13 Noise generated by a mixing layer; snapshot of source terms, levels from − 1.8 to 1.8 kg · m^{-2} · s^{-2} : a) $S_1 - \overline{S_1}$, b) $S_2 - \overline{S_2}$, c) $\overline{S_1}$, and d) $\overline{S_2}$.

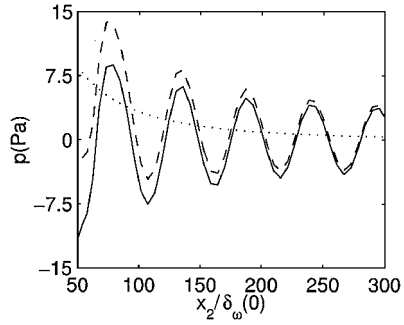

Fig. 14 Noise generated by a mixing layer; transverse pressure profiles obtained at $x_1 = 90\delta_\omega(0)$ by solving LEE with source terms: ——, $S_i - \overline{S_i}$, - - -, S_i, and · · · ·, $\overline{S_i}$.

To understand this, we consider the integral solution of Lighthill's equation in three-dimensional free space, writing the density field as

$$\rho(\boldsymbol{x}, t) - \rho_0 = \frac{1}{4\pi c_0^2} \int_{V_s} \frac{1}{|\boldsymbol{x} - \boldsymbol{y}|} \frac{\partial^2 T_{ij}}{\partial y_i \partial y_j} \left(\boldsymbol{y}, t - \frac{|\boldsymbol{x} - \boldsymbol{y}|}{c_0} \right) \mathrm{d}\boldsymbol{y}$$

where T_{ij} is Lighthill's tensor, $T_{ij} = \rho u_i u_j$, in a unheated flow at a high Reynolds number, and V_s is the sound source volume. The time average of Lighthill's tensor $\overline{T_{ij}}$ induces a density field given by

$$\bar{\rho}(\boldsymbol{x}) - \rho_0 = \frac{1}{4\pi c_0^2} \int_{V_s} \frac{1}{|\boldsymbol{x} - \boldsymbol{y}|} \frac{\partial^2 \overline{T_{ij}}}{\partial y_i \partial y_j} (\boldsymbol{y}) \, \mathrm{d}\boldsymbol{y}$$

and using properties of the convolution product

$$\bar{\rho}(\boldsymbol{x}) - \rho_0 \simeq \frac{1}{4\pi c_0^2} \frac{\partial^2}{\partial x_i \partial x_j} \left(\frac{1}{x} \right) \int_{V_s} \overline{T_{ij}}(\boldsymbol{y}) \, \mathrm{d}\boldsymbol{y}$$

as $x \to \infty$. Therefore, in the far field, this steady compressible field decreases as $1/x^3$, faster than acoustic waves, and is negligible. This reasoning has been made in three dimensions for simplicity, but a similar behavior is expected in two dimensions. To get the correct radiated field in the near field, it is thus recommended to subtract the time average of source terms introduced into LEE.

4. Results

LEE are now solved with the source term given by expression (2), and the calculated dilatation field is compared with the LES result in Fig. 15. Recall that the mean velocity field provided by LES is used to linearize Euler's equations and that the term $\boldsymbol{H}$ is canceled. The

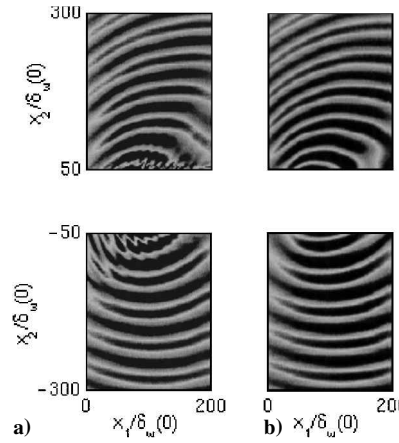

Fig. 15 Noise generated by a mixing layer; snapshots of the dilatation field obtained at the same time, levels from − 1.4 to 1.4 s^{-1}: a) from LEE with source terms (2) and b) by LES.

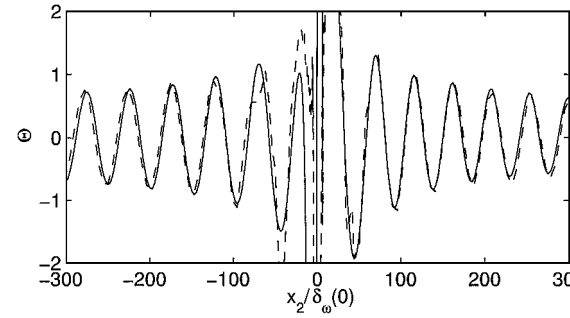

Fig. 16 Noise generated by a mixing layer; transverse dilatation profiles obtained at the pairing location $x_1 = 70\delta_\omega(0)$: - - -, from LEE with source term (2) and ——, by LES.

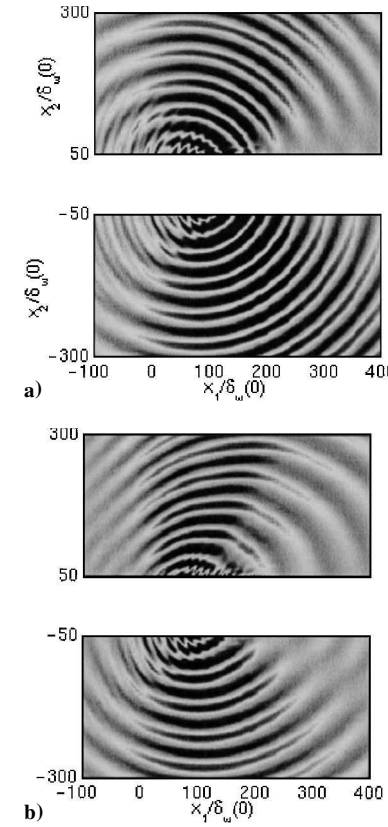

Fig. 17 Noise generated by a mixing layer; snapshots of the dilatation field obtained by solving LEE, levels from − 1.4 to 1.4 s^{-1}: a) without taking into account mean flow by setting $\bar{u}_1 = \bar{u}_2 = 0$ in LEE and b) with the mean flow in LEE.

two acoustic fields are quite consistent, and this point is made clear in Fig. 16 by comparison of corresponding transverse dilatation profiles. The two profiles are in excellent agreement in amplitude and in phase, except in the source region, where the acoustic field is greatly dominated by the local flowfield. Thus, the hybrid method based on LEE has provided the correct acoustic radiation for this flow configuration representative of flows usually studied. The importance of mean flow effects is shown in Fig. 17. LEE are solved using the source term (2), without mean velocity field and with the mean velocity field. Mean flow effects, especially convection effects in the upper flow, strongly affect the radiated field and are well taken into account by the wave operator.

VI. Conclusions

This study shows that an acoustic analogy based on LEE is able to provide aerodynamic noise, accounting for the major part of mean flow effects. The expression of source terms is validated without using ad hoc assumptions because both the velocity flowfield and the reference acoustic far field are given directly by solving the unsteady compressible Navier–Stokes equations. This supports the form of the source terms used in previous works[15] combining LEE with a stochastic velocity field. In this analogy, all mean flow effects on wave propagation are taken into account through the wave operator, and only noise generation is included into the source terms, which are quadratic in velocity fluctuations. Growing instability waves are removed by considering a simplified formulation of LEE, in which the mean shear term corresponding to the second derivative of the velocity profile in Rayleigh's stability equation is canceled. This modification of LEE is a good approximation of high-frequency sound propagation and does not modify propagation significantly in the low-frequency case. Further studies are also needed to analyze the associated stability equation.

Appendix A: Definition of Source Terms for LEE

The three vectors $\boldsymbol{E}$, $\boldsymbol{F}$, and $\boldsymbol{H}$ of LEE (1) written in the following two-dimensional conservative form:

$$\frac{\partial \boldsymbol{U}}{\partial t}+\frac{\partial \boldsymbol{E}}{\partial x_1}+\frac{\partial \boldsymbol{F}}{\partial x_2}+\boldsymbol{H}=\boldsymbol{S}$$

are given, respectively, by

$$\boldsymbol{E}=\begin{pmatrix}\rho'\bar{u}_1+\bar{\rho}u_1'\\ \bar{u}_1\bar{\rho}u_1'+p'\\ \bar{u}_1\bar{\rho}u_2'\\ \bar{u}_1p'+\gamma\bar{p}u_1'\end{pmatrix},\qquad \boldsymbol{F}=\begin{pmatrix}\rho'\bar{u}_2+\bar{\rho}u_2'\\ \bar{u}_2\bar{\rho}u_1'\\ \bar{u}_2\bar{\rho}u_2'+p'\\ \bar{u}_2p'+\gamma\bar{p}u_2'\end{pmatrix}$$

$$\boldsymbol{H}=\begin{pmatrix}0\\ (\bar{\rho}u_1'+\rho'\bar{u}_1)\dfrac{\partial\bar{u}_1}{\partial x_1}+(\bar{\rho}u_2'+\rho'\bar{u}_2)\dfrac{\partial\bar{u}_1}{\partial x_2}\\ (\bar{\rho}u_1'+\rho'\bar{u}_1)\dfrac{\partial\bar{u}_2}{\partial x_1}+(\bar{\rho}u_2'+\rho'\bar{u}_2)\dfrac{\partial\bar{u}_2}{\partial x_2}\\ (\gamma-1)p'\nabla\cdot\bar{u}-(\gamma-1)\boldsymbol{u}'\cdot\nabla\bar{p}\end{pmatrix}$$

The term $\boldsymbol{H}$ is zero for a uniform mean flowfield. It contains a part of the refraction effects. The vector $\boldsymbol{S}=(0, S_1, S_2, 0)^t$ is a possible aerodynamic source term.

To derive a wave equation on the pressure fluctuation p' including all acoustic–mean flow interactions, LEE must be combined to eliminate all of the terms involving velocity fluctuations. In this way, the simplest nontrivial differential equation written on the pressure is obtained in the case of a strictly parallel mean flow, with $\bar{u}_1=\bar{u}_1(x_2)$ and $\bar{u}_2=0$. Because the steady mean flow satisfies Euler's equations, the mean pressure is necessarily constant with $\bar{p}=p_0$, whereas the mean density and speed of sound are only function of the transverse coordinate x_2, $\bar{\rho}=\bar{\rho}(x_2)$, and $\bar{c}=\bar{c}(x_2)$. Moreover, entropy fluctuations are simply convected by the mean flow without production, and if we assume no entropy fluctuation at a given time, then $p'\simeq\bar{c}^2\rho'$. Applying the convective derivative based on the mean flow velocity $\bar{\mathrm{D}}/\bar{\mathrm{D}}t=\partial/\partial t+\bar{u}_1\partial/\partial x_1$ to the continuity equation, taking the divergence of the momentum equation, and subtracting the two expressions lead to Phillips' wave equation:

$$\frac{1}{\bar{c}^2}\frac{\bar{\mathrm{D}}^2p'}{\bar{\mathrm{D}}t^2}-\nabla^2p'-2\bar{\rho}\frac{\partial u_2'}{\partial x_1}\frac{\mathrm{d}\bar{u}_1}{\mathrm{d}x_2}=-\nabla\cdot\boldsymbol{S}\qquad\text{(A1)}$$

To eliminate the term linear in u_2', the operator $\bar{\mathrm{D}}/\bar{\mathrm{D}}t$ is again applied to Eq. (A1). Using an appropriate combination of the resulting expression with the transverse momentum equation differentiated with respect to x_1, one finds

$$\frac{\bar{\mathrm{D}}}{\bar{\mathrm{D}}t}\left[\frac{1}{\bar{c}^2}\frac{\bar{\mathrm{D}}^2p'}{\bar{\mathrm{D}}t^2}-\nabla^2p'\right]+2\frac{\mathrm{d}\bar{u}_1}{\mathrm{d}x_2}\frac{\partial^2p'}{\partial x_1\partial x_2}=\Lambda\qquad\text{(A2)}$$

where the source term is

$$\Lambda=-\frac{\bar{\mathrm{D}}}{\bar{\mathrm{D}}t}\nabla\cdot\boldsymbol{S}+2\frac{\mathrm{d}\bar{u}_1}{\mathrm{d}x_2}\frac{\partial S_2}{\partial x_1}$$

Equation (A2) is derived from LEE using the fluctuating pressure[25] for simplicity, but a similar equation could be obtained with the logarithmic pressure. It takes the form of Lilley's wave equation whose an unambiguous interpretation can be provided only for a unidirectional sheared mean flow. In this case, Goldstein[25] has given a simplified formulation of Lilley's equation, recently supported by DNS results of Colonius et al.[12] To make Eq. (A2) closely correspond to Goldstein's simplified equation, the source term Λ must be written as

$$\Lambda=\frac{\bar{\mathrm{D}}}{\bar{\mathrm{D}}t}\frac{\partial^2\rho u_i'u_j'}{\partial x_i\partial x_j}-2\frac{\mathrm{d}\bar{u}_1}{\mathrm{d}x_2}\frac{\partial^2\rho u_2'u_j'}{\partial x_1\partial x_j}\qquad\text{(A3)}$$

See, in particular, expressions (1.22) and (6.24) in Ref. 25 corresponding, respectively, to LEE and the simplified Lilley equation. As a consequence, the corresponding source terms in LEE are given rigorously by

$$S_i=-\frac{\partial\rho u_i'u_j'}{\partial x_j}$$

Appendix B: Simplified LEE

The simplified wave operator used in Sec. V to avoid the growth of instability waves is obtained by cancelling the vector $\boldsymbol{H}$ in LEE. This vector is written as $[0, \bar{\rho}u_2'\,\mathrm{d}\bar{u}_1/\mathrm{d}x_1, 0, 0]^t$ for a strictly parallel mean flow. The effects of the removal of $\boldsymbol{H}$ on Rayleigh's equation governing instability waves and on sound propagation are of interest.

Instability waves are governed by the homogeneous LEE (1). For a strictly parallel mean flow $\bar{u}_1=\bar{u}_1(x_2)$, assuming incompressible perturbations to keep the problem as simple as possible and writing the transverse velocity u_2' as the real part of $\hat{u}_2(x_2)\exp[i(kx_1-\omega t)]$, Rayleigh's stability equation is given by

$$\left(\bar{u}_1-\frac{\omega}{k}\right)\left[\frac{\mathrm{d}^2\hat{u}_2}{\mathrm{d}x_2^2}-k^2\hat{u}_2\right]-\frac{\mathrm{d}^2\bar{u}_1}{\mathrm{d}x_2^2}\hat{u}_2=0\qquad\text{(B1)}$$

For spatial stability analysis, the axial wave number $k=k_r+ik_i$ is complex, whereas the angular frequency ω is real. Thus, perturbations are unstable when the imaginary part of the wave number is negative, for $k_i<0$.

The new stability equation corresponding to the simplified LEE is written as

$$\left(\bar{u}_1-\frac{\omega}{k}\right)\left[\frac{\mathrm{d}^2\hat{u}_2}{\mathrm{d}x_2^2}-k^2\hat{u}_2\right]+\frac{\mathrm{d}\bar{u}_1}{\mathrm{d}x_2}\frac{\mathrm{d}\hat{u}_2}{\mathrm{d}x_2}=0\qquad\text{(B2)}$$

and the associated homogeneous wave equation is

$$\frac{\bar{\mathrm{D}}}{\bar{\mathrm{D}}t}\left[\frac{1}{\bar{c}^2}\frac{\bar{\mathrm{D}}^2p'}{\bar{\mathrm{D}}t^2}-\nabla^2p'\right]+\frac{\mathrm{d}\bar{u}_1}{\mathrm{d}x_2}\frac{\partial^2p'}{\partial x_1\partial x_2}=\Lambda\qquad\text{(B3)}$$

Compare the two new equations [Eqs. (B2) and (B3)] to the classical ones for full LEE [Eqs. (B1) and (A2), respectively]. The second derivative of the mean velocity $\bar{u}_1$ does not appear in Eq. (B2) governing instability wave developments. This term plays a crucial

role in Rayleigh's equation (B1) with the inflexion point theorem. No simple rule can be applied for the stability analysis of simplified LEE, but this formulation seems to be stable in our numerical experiences as well as in the numerical tests performed by one of the referees. The consequence for acoustic propagation of the removal of $\boldsymbol{H}$ is that the refraction term proportional to $\mathrm{d}\bar{u}_1/\mathrm{d}x_2$ in Eq. (B3) differs by a factor two with respect to Lilley's Eq. (A2). This term becomes small compared to the higher derivative terms as the frequency increases.[11,25] Thus, Eq. (B3) is a good approximation for the high-frequency case. The low-frequency case is more ambiguous, and to clarify this point, a numerical example is provided in Appendix C.

Appendix C: Sound Propagation Problem Solved by Simplified LEE

The response of simplified LEE to time-harmonic forcing of the mixing layer mean flow studied in Sec. V is now investigated. The mean axial velocity is expressed as

$$\bar{u}_1(x_1, x_2) = (U_1+U_2)/2+[(U_2-U_1)/2]\tanh[2x_2/\delta_\omega(x_1)] \quad \text{(C1)}$$

where the vorticity thickness is taken as

$$\delta_\omega(x_1) = \delta_\omega(0)\left\{\tfrac{3}{2}+\tfrac{1}{2}\tanh[(x_1-70)/10]\right\}$$

to fit the LES result shown in Fig. 12. The vector $\boldsymbol{S}$ represents a monopolar source:

$$\boldsymbol{S} = \epsilon\sin(\omega t)\exp\left[-\ell n(2)\frac{\left(x_1^2+x_2^2\right)}{b^2}\right]\begin{bmatrix}1/c_0^2\\0\\0\\1\end{bmatrix}$$

with the angular frequency $\omega = 2\pi f_p$ corresponding to the vortex pairing frequency, located at $x_1 = 70\delta_\omega(0)$. The amplitude of the source is $\epsilon = 10^{-4}$. The half-width of the Gaussian profile is $b = 3\times\Delta$, $\Delta = 0.24\delta_\omega(0)$ being the step size in the shear region. The mesh grid is composed of 651×501 points to obtain a computational domain similar to the domain used in Sec. V, but larger in the downstream direction to avoid growing instability waves reaching the outflow boundary conditions and then deteriorating the acoustic field.

The pressure field obtained by solving simplified LEE is represented in Fig. C1. Waves fronts are ovalized by the two uniform flows U_i by convection effects, and no instability waves are observed. The difference between the pressure fields provided by simplified LEE and full LEE is plotted in Fig. C2. As expected, using full LEE, instability waves are generated and convected in the downstream direction. Resulting errors for the acoustic field are limited to two opposite regions close to the flow axis, where refraction effects appear typically for a sheared mean flow. However, they are small, with a difference of one order of magnitude with respect to the acoustic field, in spite of a ratio $\lambda_p/\delta_\omega(0) = 51.5$. Transverse pressure profiles obtained upstream and downstream from the monopolar source at $x_1 = 0$ and $300\delta_\omega(0)$ are shown in Fig. C3 and confirm more quantitatively the good approximation of sound propagation even in this low-frequency case.

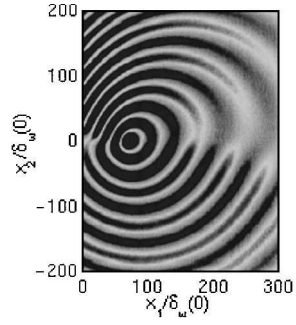

Fig. C1 Monopolar source in a sheared mean flow; pressure field obtained using simplified LEE with $\boldsymbol{H}=\mathbf{0}$, levels from -2.6×10^{-6} to 2.6×10^{-6}.

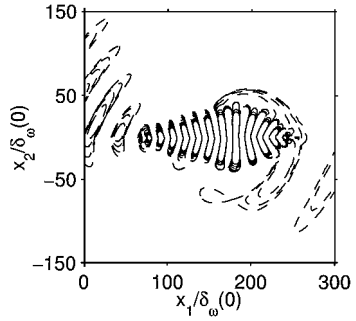

Fig. C2 Monopolar source in a sheared mean flow; difference between the pressure fields obtained using simplified LEE and full LEE, contours: – – –, $[0.5, 1, 2, 4]\times10^{-7}$ and ——, $[1, 2, 4]\times10^{-6}$.

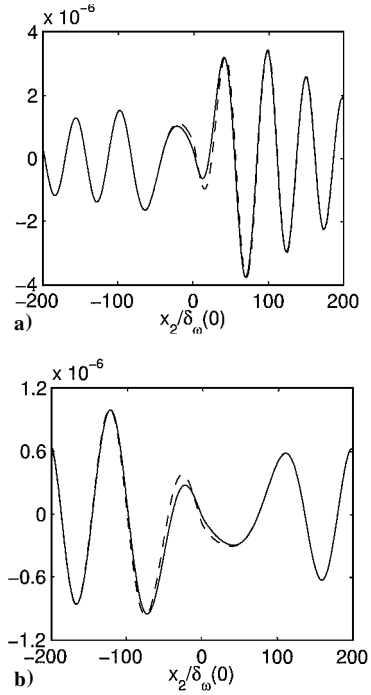

Fig. C3 Monopolar source in a sheared mean flow; transverse pressure profiles obtained using ——, simplified LEE and – – –, full LEE: a) $x_1 = 0$ and b) $x_1 = 300\delta_\omega(0)$.

Acknowledgments

Computing time was provided by Institut du Développement et des Ressources en Informatique Scientifique (Centre National de la Recherche Scientifique). We gratefully acknowledge Philippe Lafon from Electricité de France for stimulating discussions and for financial support. We would like to thank the three referees for helpful comments.

References

[1] Freund, J. B., "Acoustic Sources in a Turbulent Jet: A Direct Numerical Simulation Study," AIAA Paper 99-1858, May 1999.

[2] Colonius, T., "Lectures on Computational Aeroacoustics," Lectures Series 1997-07, von Karman Inst. for Fluid Dynamics, Rhode-Saint-Genese, Belgium, 1997.

[3] Bogey, C., "Calcul direct du bruit aérodynamique et validation de modèles acoustiques hybrides," Ph.D. Dissertation, No. 2000-11, Ecole Centrale de Lyon, Ecully, France, 2000.

[4] Bogey, C., Bailly, C., and Juvé, D., "Large Eddy Simulation of a Subsonic Jet: Direct Calculation of Its Radiated Sound Field," AIAA Paper 2000-2009, June 2000.

[5] Lighthill, M. J., "On Sound Generated Aerodynamically—I. General Theory," *Proceedings of the Royal Society of London, Series A: Mathematical and Physical Sciences*, London, Vol. 211, Ser. 1107, 1952, pp. 564–587.

[6] Ribner, H. S., "Effects of Jet Flow on Jet Noise via an Extension to the Lighthill Model," *Journal of Fluid Mechanics*, Vol. 321, 1996, pp. 1–24.

[7] Bogey, C., Bailly, C., and Juvé, D., "Noise Computation Using Lighthill's Equation with Inclusion of Mean Flow–Acoustics Interactions," AIAA Paper 2001-2255, May 2001.

[8] Lilley, G. M., "The Generation and Radiation of Supersonic Jet Noise. Vol. 4—Theory of Turbulence Generated Jet Noise, Noise Radiation from Upstream Sources, and Combustion Noise. Part II: Generation of Sound in a Mixing Region," U.S. Air Force Aeropropulsion Lab., AFAPL-TR-72-53, Vol. 4, Wright–Patterson AFB, OH, 1972.

[9]Pridmore-Brown, D. C., "Sound Propagation in a Fluid Flowing Through an Attenuating Duct," *Journal of Fluid Mechanics*, Vol. 4, 1958, pp. 393–406.

[10]Goldstein, M. E., "Aeroacoustics of Turbulent Shear Flows," *Annual Review of Fluid Mechanics*, Vol. 16, 1981, pp. 263–285.

[11]Candel, S. M., "Numerical Solution of Conservation Equations Arising in Linear Wave Theory: Application to Aeroacoustics," *Journal of Fluid Mechanics*, Vol. 83, No. 3, 1977, pp. 465–493.

[12]Colonius, T., Lele, S. K., and Moin, P., "Sound Generation in a Mixing Layer," *Journal of Fluid Mechanics*, Vol. 330, 1997, pp. 375–409.

[13]Berman, C., and Ramos, J., "Simultaneous Computation of Jet Turbulence and Noise," AIAA Paper 89-1091, 1989.

[14]Béchara, W., Bailly, C., Lafon, P., and Candel, S., "Stochastic Approach to Noise Modeling for Free Turbulent Flows," *AIAA Journal*, Vol. 32, No. 3, 1994, pp. 455–463.

[15]Bailly, C., Lafon, P., and Candel, S., "A Stochastic Approach to Compute Noise Generation and Radiation of Free Turbulent Flows," AIAA Paper 95-092, June 1995.

[16]Longatte, E., Lafon, P., and Candel, S., "Computation of Noise Generation in Internal Flows," AIAA Paper 98-2332, May 1998.

[17]Bailly, C., and Juvé, D., "A Stochastic Approach to Compute Subsonic Noise Using Linearized Euler's Equations," AIAA Paper 99-1872, May 1999.

[18]Tam, C. K. W., and Webb, J. C., "Dispersion-Relation-Preserving Finite Difference Schemes for Computational Acoustics," *Journal of Computational Physics*, Vol. 107, 1993, pp. 262–281.

[19]Tam, C. K. W., and Dong, Z., "Radiation and Outflow Boundary Conditions for Direct Computation of Acoustic and Flow Disturbances in a Nonuniform Mean Flow," *Journal of Computational Acoustics*, Vol. 4, 1996, pp. 175–201.

[20]Bogey, C., Bailly, C., and Juvé, D., "Numerical Simulation of the Sound Generated by Vortex Pairing in a Mixing Layer," *AIAA Journal*, Vol. 38, No. 12, 2000, pp. 2210–2218.

[21]Bailly, C., and Juvé, D., "Numerical Solution of Acoustic Propagation Problems Using Linearized Euler's Equations," *AIAA Journal*, Vol. 38, No. 1, 2000, pp. 22–29.

[22]Lee, D. J., and Koo, S. O., "Numerical Study of Sound Generation Due to a Spinning Vortex Pair," *AIAA Journal*, Vol. 33, No. 1, 1995, pp. 20–26.

[23]Powell, A., "Theory of Vortex Sound," *Journal of the Acoustical Society of America*, Vol. 36, No. 1, 1964, pp. 177–195.

[24]Mitchell, B. E., Lele, S. K., and Moin, P., "Direct Computation of the Sound from a Compressible Co-Rotating Vortex Pair," *Journal of Fluid Mechanics*, Vol. 285, 1995, pp. 181–202.

[25]Goldstein, M. E., *Aeroacoustics*, McGraw–Hill, New York, 1976, Eqs. (1.22) and (6.24), pp. 9, 257.

P. J. Morris
Associate Editor